

Effect of Process Parameters on the Recycled Ageing Polyamide-12 Tensile Strength in Selective Laser Sintering (SLS)

Irfan Ur Rahman^a, Norfariza Ab Wahab^{b,*}, Mohd Idain Fahmy Rosley^b, Lailatul Harina Paijan^c, Ranjit Singh^e and Mohd Fauzi Mamat^b

^aDepartment of Manufacturing Engineering, Faculty of Manufacturing Engineering, Universiti Teknikal Malaysia Melaka, Hang Tuah Jaya, 76100 Durian Tunggal, Melaka, Malaysia

^bDepartment of Mechanical Engineering Technology, Faculty of Mechanical and Manufacturing Engineering Technology, Universiti Teknikal Malaysia Melaka, Hang Tuah Jaya, 76100 Durian Tunggal, Melaka, Malaysia

^cDepartment of Industrial Technology, Faculty of Mechanical and Manufacturing Engineering Technology, Universiti Teknikal Malaysia Melaka, Hang Tuah Jaya, 76100 Durian Tunggal, Melaka, Malaysia

^dDepartment of Electronics & Computer Engineering Technology, Universiti Teknikal Malaysia Melaka, Malaysia

*Corresponding author. Tel.: +6-0192608712; e-mail: norfariza@utem.edu.my

ABSTRACT

Selective laser sintering (SLS) applications are rapidly growing in various sectors such as automobile, aeronautics, biomedical and custom consumer products. The properties of SLS made parts exhibit high dependence on the settings of process parameters, which can be improved by choosing and adjusting sintering conditions accurately. This paper presents research work for evaluating the effect of process parameters on the tensile properties of the part manufactured on Farsoon SS402P SLS from recycled ageing FS 3300PA which is PA-12 based powder and standard operating parameters using Response Surface Methodology (RSM) design of experiments. Typically, the recommendation from the manufacturer's laser power is 70watt. The research is designed to fabricate the parts by SLS with three-part arrangements i.e. (0-degree XY/Y, 90-degree YZ/Y and 180-degree YZ/Y) by three different value of laser power, which are 67.5watt, 70watt, and 72.5watt with different values of layer thickness i.e. (0.09mm, 0.12mm and 0.15mm). Comparison have been made between the virgin powder and recycled power regarding tensile result. Tensile tests have been performed as per the ASTM D638 standard using recommendations from ISO/ASTM 52921. According to the results, effect of laser power is successfully analyzed by employing tensile strength test.

Keywords: *Selective laser sintering, PA 12, Tensile properties, Orientation*

1. INTRODUCTION

Selective laser sintering (SLS), an additive manufacturing technique, makes it possible to produce complicated parts without the use of tools, making it possible to produce personalized goods at a reasonable price even in small batches. In contrast to this benefit, the producible component dimension is currently constrained. Due to the size of the building chamber in commercial SLS systems, this restriction exists. Additionally, a lot of the expensive polyamide 12 powder is required to produce big SLS parts. Reliable joining techniques that enable excellent mechanical binding qualities in assemblies are essential for SLS components to get beyond these restrictions [1]. PA-12 has been chosen as the research's raw material, while Selective Laser Sintering (SLS) has been selected as the manufacturing procedure. The usage of a wide variety of polymeric powder materials, particularly composites based on polymers like Polyamide 12 (PA-12), Polyether Ether Ketone (PEEK), Polyethylene (PE), Polycarbonates (PC), and

Polystyrene (PS), has been documented regularly. The classification of materials for SLS is depicted in Figure 1. According to the so-called pyramid of polymeric materials at Figure 1(b) and the inorganic or polymeric content at Figure 1(a) for additive manufacturing [2].

Due to the unsatisfactory processing behaviour and performance of the final product, all of them save PA-12 have failed commercially. Figure 2 displays three different images of the powder morphology during laser sintering. Figure 2(a) depicts cryogenically processed, rough PA-11 powder; Figure 2(b) depicts a potato-shaped PA-12 powder precipitate from an ethanol solution, and Figure 2(c) depicts spherical PS powder formed via emulsion polymerization [2]. Component quality and outcomes are significantly influenced by material characteristics such as particle size distribution, crystallinity, powder flowability, melting temperature, and melt viscosity as well as process variables such as faster rate and path, laser power, and ambient bed temperature [3].

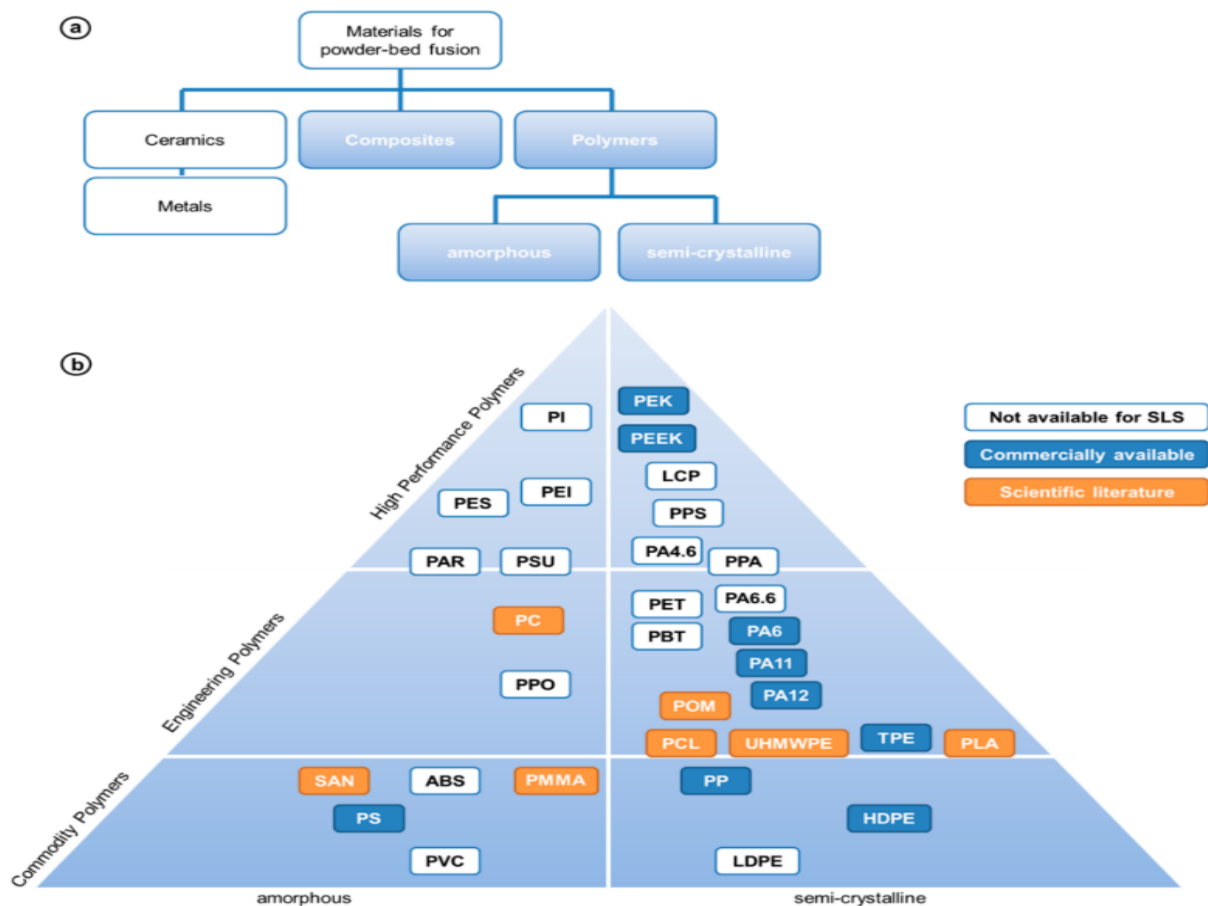


Figure 1. Classification of materials for SLS.

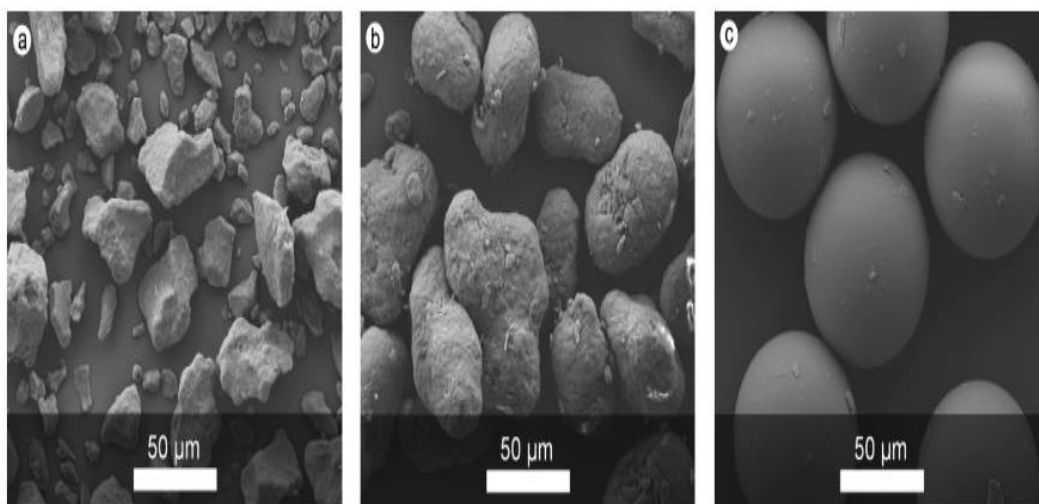


Figure 2. Morphology of laser sintering powder.

Laser processing settings have an impact on the sintering procedure as well as product characteristics (surface roughness, dimensional accuracy, tensile properties, flexural properties, and manufacturing time). Processing settings can be altered individually for the product's internal layers (hatching) and external layers (object contour). How much high energy density fuel is put into the reactor determines the mechanical qualities of the end product. Energy density can be used to determine processing conditions from published research and independent experimentation [4]. Low mechanical strength

of the printed structure was caused by high laser speeds that shorten the time the powder is exposed to the beam. SLS printability was altered by the laser energy density (ED), which changed the temperature of the powder bed [5].

This study aims to investigate the effects of different process parameters on the mechanical properties of PA 12 using the SLS printed samples. These printed parts' properties are essential in both manufacturing and prototyping applications and are mainly influenced by the process parameters.

2. THEORETICAL BACKGROUND

Selective laser sintering, which uses a laser to connect successive layers of powder, is one method for incrementally producing models and prototypes [6]. The advantage of this method is the capability of obtaining a model of any shape without the necessity of bringing the material to a liquid state [7]. The working chamber of a machine outfitted with a computer that regulates the manufacturing process is where the entire laser sintering procedure takes place. Depending on the material being utilized, specialized software enables control and adjustment of the pressure value and atmosphere present inside the chamber [8, 9]. Infrared laser energy from a CO₂ (10.6 m) or Nd:YAG (1.06 m) laser is used for this procedure [10, 11]. Spreading a thin layer of powder on a table that can be moved along the Z axis is the foundation of selective laser sintering. The substrate for the thing being generated is this layer. According to input and appropriately configured data regarding subsequent layers in the cross-section of the object's spatial image, the laser beam moves across the powder's surface [12]. The right laser beam characteristics can be chosen to melt or sinter powder particles in precisely specified regions. Next, the platform's framework and the table are lowered from their prior positions by a predetermined height (often equivalent to the thickness of one layer; 30 to 100 m), and a second thin coating of powder is dispersed [13]. The blade for removing extra material returns to its previous position after the excess powder is routed into a collection box outside the platform on which things are built. The cross-section is once more scanned by the laser. Until a cohesive item is obtained in accordance with the information in the generated digital file, this process is repeated.

Within the scope of the SLS Rapid Prototyping process, the two forms of laser sintering—indirect and direct—can be separated [14]. Indirect selective laser sintering (ISLS, Fig. 3) makes use of metallic powder that has been 5 m thickly covered with polymer. The metallic powder grains are unaltered as the polymer layer is sintered by the laser beam. Due to the low strength qualities and large porosity (even exceeding 50%) of an object created using this approach, additional heat processing is required [15]. The two stages of thermal treatment are polymer removal and infiltration. The polymer evaporates because of high temperature. Sintering is the process of creating necks between metal particles as temperature is raised further. The following phase is infiltration, which is based on either continuing to sinter until complete density is attained or filling any remaining pores after polymer evaporation with metal with a low melting point [16, 17]. Additionally, infiltration enables the creation of composites with specified properties if pores are filled with a different metal [18].

3. MATERIAL AND METHODS

3.1. Parts Preparation and Procedure

In this research parts have been fabricated by Farsoon SS402P. The material used in this research is recycled aged powder of polyamide 12. The part orientations were 0-degree xy/y, 90-degree yz/y and 180-degree yz/y as shown in figure 3. The parts have been fabricated with different laser power 67.5watt, 70watt and 72.5watt and with three values of layer thickness (0.09mm, 0.12mm and 0.15mm), to investigate the effect of process parameters on the tensile properties of polyamide 12 aged material. This result will also be compared with virgin powder to draw an authentic conclusion for the industrial applications.

Specimen have been prepared as per the ASTM D638 – 10 standard [19]. Its orientation with respect to the coordinate axes are chosen according to the RSM design of experiment and the sequence of orientation is fixed as first about X axis then about Y and then about Z axis. The minimum angle is obviously kept 0-degree and the maximum angle is kept as 180-degree, as the larger angles will be one of the symmetrical conditions between 0 to 180-degree. Figure 4. presents the tensile test carried out on the five specimens printed with the SLS 3D printer by universal testing system Shimadzu AG-100KN PLUS.

3.2. Polyamid-12 (PA-12) Recycled Ageing Material

PA-12-based powder made from recycled, aged FS 3300PA will be used in this research. The term "recycled ageing PA-12" refers to a non-sintered powder that underwent extreme thermal stress after being repeatedly heated in a chamber below melting point over an extended length of time [19]. This used aging powder originates from areas that experience significant heat, such as the surface's bottom [20]. Under a scanning electron microscope (SEM), Figures 5 and 6 illustrate the form differences between virgin (a), aged (b), and severely aged PA-12 SLS powder (c). The two recycled ageing powders have similar sizes, averaging between 55 and 60 m. However, a closer examination of the aging SLS powder particles revealed significant cracking, which occurred because of the powder's continual exposure to high temperatures and massive thermal stress in the chamber during the sintering process. The evaporation of any leftover alcohol, the absorption of moisture, and the subsequent expansion/shrinkage phases of the process cycles are likely causes of the cracking problem, albeit their exact reason is yet unknown [20]. Due to the powder's increasing molecular weight, these morphological changes may cause the melt flow rate of the material to decrease from above 50g/10min for virgin fresh powder to less than 18g/10min.

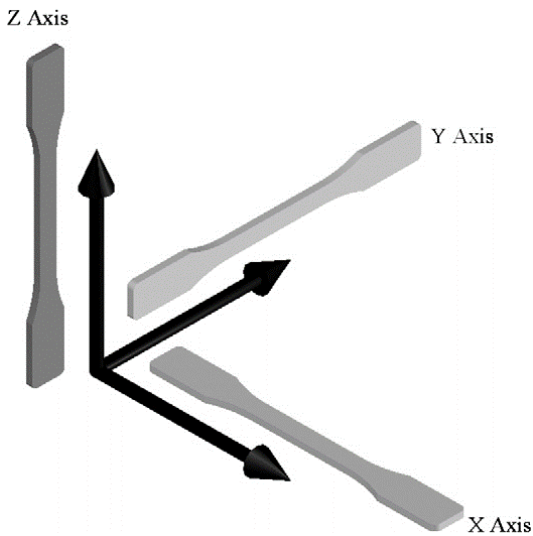


Figure 3. Part arrangement during sintering process.



Figure 4. Universal testing system Shimadzu AG-100KN PLUS.

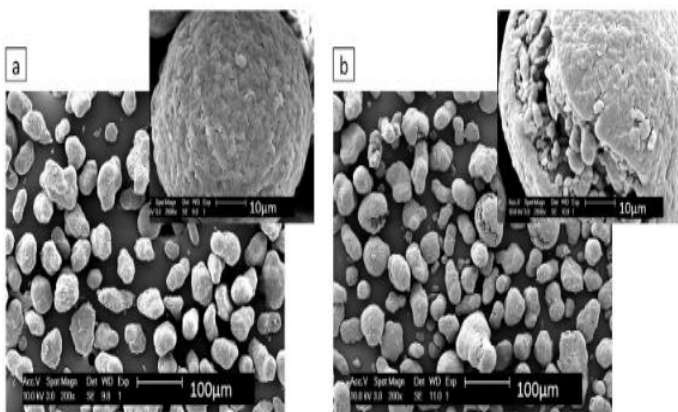
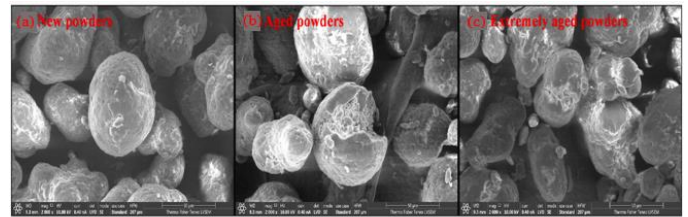
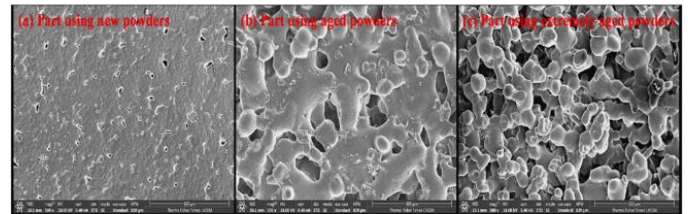


Figure 5. SEM images of (a) virgin and (b) aged PA12 powder.



(a) Polyamide 12 powder samples



(b) Polyamide 12 part samples

Figure 6. SEM images of powders (a) and parts from PA-12 powders (b).

3.3. Farsoon SS402P Selective Laser Sintering (SLS) Machine

The industrial grade Farsoon SS402P Selective Laser Sintering (SLS) machine has been chosen for use. The Selective Laser Sintering (SLS) Laboratory FTKMP at Universiti Teknikal Malaysia Melaka (UTeM) is home to a Farsoon model SS402P SLS 3D printer. The SLS machine weighs 3000 kg and has external dimensions measuring 2660 mm by 1540 mm by 2150 mm. The SLS chamber can accommodate builds up to 400mm by 400mm by 450mm, with an effective build size of 350mm by 350mm by 430mm. With a maximum output of 100W and a scanning speed of 12.7m/s, CO₂ is used as a laser. Each rotating roller has a 0.1mm coating of powder and a 0.3mm laser wavelength [21].



Figure 7. Farsoon SS402P Selective Laser Sintering (SLS) machine.

3.4. Response Surface Methodology (RSM)

The examination of the impact of distinct independent parameters on the defined quality attributes is provided by the optimization of process parameters by Design of Experiment (DOE). DOE can be used to strengthen processes and products. The Taguchi Method, Response Surface Method, and Factorial Designs are a few techniques utilized in experiment design. Response surface analysis

the relationship between the input process parameters and the response variable (output) is explored using the statistical and mathematical technique known as the response surface methodology. In 1951, George E. P. Box and K. B. Wilson introduced this technique. To get the best result, RSM designs trials in a sequential order. This approach aids in creating, enhancing, and optimizing the process parameters [22-23].

Sudhir Kumar, Pradeep Kumar and H. S. Shan[24] examined the impact of process variables on the solidification time of Al-7%Si alloy produced by vacuum assisted evaporative pattern casting technique, such as vacuum level, pouring temperature, grain fineness number, amplitude of vibration and time of vibration. In experiments, the central composite rotatable design has been used. 32 tests must be run since there are 5 elements or variables, and RSM is used to build a second order response mathematical model. Here, it is observed that the solidification time reduces as the vacuum level, vibrational amplitude, and vibrational time rise. M. Manohar, Jomy Joseph, T. Selvaraj and D. Sivakumar [25] examined how turning Inconel 718 alloy input parameters such cutting speed, feed, and depth of cut affected the rate of material removal. Here, the 15 experiments are planned to use the Box Behnken Design method. To understand the relationship between input and output parameters, a polynomial model was created. ANOVA is then conducted in more detail. M. V. Satish Kumar and M. Pradeep Kumar [26] optimized CNC turning parameters for MRR and surface roughness when working with EN 19 alloy steel. For experiment design, a face-centered central composite RSM was utilized, and an ANOVA was used to identify the significant factor influencing the result. Additionally, using Minitab 17 software, regression analysis and a desirability method were performed.

3.4.1. Design Expert

Design Expert is software a statistical method produced by Stat ease. This was first released in 1996 to help carry out experimental designs such as determining the optimum formula for a preparation. Apart from optimization, software can also interpret the factors in the experiment. In software, it is divided into three choices of research directions depending on the experimental design to be carried out. There are screening, characterization, and optimization options. Screening requires the least amount of run but provides the least amount of information. Run is the number of experiments that must be carried out according to the selected experimental design. Screening is used if there are many possible factors (>6), but it is not known which one has a real effect. Identification of several important factors using only two levels of each factor and estimates of the main effect (no interaction). Requires follow-up with 2nd DOE to estimate interactions and further requirements [27]. Table 1 shows data only for 72.5watt and 012mm.

3.4.2. Box-Behnken Design

In this research Box-Behnken design is selected, as the designs have fewer runs than 3-Level factorials, so it shows a total of 17 runs for three factors i.e. (laser power, layer thickness and orientation as shown in Table 2. Comparisons between BBD and other responsive surface designs (centre composite design, Doehlert matrix and full three-level factorial design) demonstrated that the BBD and Doehlert designs are slightly more efficient than central composite design, but much more efficient than three level full factorial design where the efficiency of the experimental design is determined by the number of coefficients in the estimated model divided by the number of trials [28].

4. RESULT AND DISCUSSION

4.1. Modeling of Tensile strength by ANOVA and RSM

The results of the tensile strength test were collected and used to generate a representative mathematical model. Statistical processing and ANOVA were adopted to obtain reliable mathematical models based on the previously described procedures and experimental data, obtained. The significance of the model and the members of the response polynomial was determined with ANOVA. Table 3 presents the data of the initial ANOVA analysis, with a recommendation for selection of the appropriate model for the tensile strength prediction.




A quadratic model for the tensile strength prediction was proposed, based on the recommendation for the selection of the appropriate model, which is the selection of highest order polynomial where the additional terms are significant and the model is not aliased. The cubic model has more terms than the number of unique points in the design, because some terms were aliased, and the model was aliased. Table 4 presents ANOVA analysis for quadratic model.

The Model F-value of 18.82 implies the model is significant. There is only a 0.04% chance that an F-value this large could occur to noise. P-value less than 0.0500 indicate model terms are significant. In this case B, C, B², C² are significant model terms. Values greater than 0.1000 indicate the model terms are not significant. If there are many insignificant model terms (not counting those required to support hierarchy), model reduction may improve your model.

4.2. Tensile Strength

The following graphs are generated by RSM analyses. Figure 8(a) represents the tensile strength vs Laser power which shows the highest value 39.4278Mpa of tensile strength at the laser power 72.5 watt. Conversely, the lowest value of tensile strength is 8.1023Mpa at 67.5watt. It is depicted from Figure 8(a) that higher the laser power, increase the tensile strength. The size of the laser power affects the amount of energy absorbed by the powder. When the laser power is small, the formed part is looser, less compact and less tensile due to insufficient energy. When the laser power increases, the compactness of the formed part increases

Table 1 Tensile testing result for each sample

Parts Name	No.	Tensile strength	Average	Elongation	Average	Parts after testing
72.5watt 0.12mm 0-degree	1	30.2974	24.5723	16.4000	16.8374	
	2	31.2841		17.2034		
	3	31.3884		14.8514		
	4	28.8412		15.5885		
	5	32.4388		20.1441		
90-degree	1	30.4232	30.9981	18.8107	17.5439	
	2	30.9571		18.4427		
	3	31.4930		17.4737		
	4	31.1837		15.4160		
	5	30.9337		17.5767		
180-degree	1	6.39087	9.7532	1.19479	2.2724	
	2	12.9282		3.56501		
	3	11.0763		2.43945		
	4	10.3773		2.35242		
	5	7.99372		1.81078		

due to the increase in energy. The tensile strength is increased [29]. Figure 8(b) represents the tensile vs layer thickness which indicates the highest tensile strength value at layer thickness 0.09mm while the lowest value is at 0.12mm. which shows that using a lower layer thickness tends to result in higher tensile strength compared to using a higher layer thickness. With lower layers, the laser energy can be focused more tightly, leading to better material fusion and in achieving a higher degree of consolidation between adjacent layers, which is essential for good tensile strength [30]. Similarly, Figure 8(c) shows the highest value of tensile strength at 90degrees while the lowest value is at 180degrees. It is also obvious from Table 1 which shows the effect of orientation on tensile strength. SLS, create parts layer by layer. In 180degrees orientation, each layer gets fused to the layer below it, and there can be weaker bonds between these layers compared to the orientations in-plane (0 and 90degrees) bonds. These weaker interlayer bonds can result in reduced tensile strength at 180degrees. Figure 8(C) shows the tensile strength is higher with 90degrees as compared to 0 and

180degrees because SLS builds parts layer by layer. In the y-axis (horizontal plane), the material fuses more consistently because it is deposited layer by layer in a continuous fashion. This results in stronger interlayer bonding and higher tensile strength. In SLS systems, the laser scans horizontally, perpendicular to the x-axis. This means that the material in the y-axis direction receives more energy from the laser, resulting in better fusion and stronger bonds [31].

4.3. Model Graph Analysis

Effect on Tensile Strength Tensile Strength Effect - Laser Power (Watt) vs Layer Thickness (mm). Refer Figure 9. Based on the graph obtained it can be concluded that the minimum 0.09mm layer thickness with the maximum 72.5watt laser power at 90-degree will gives the highest tensile strength which is 39.4278MPa. While for the minimum tensile strength, the value is 8.1023MPa generated from 0.12mm layer thickness with the minimal 67.5watt laser power at similar 180-degree orientation.

Table 2 RSM design using the Box-Behnken

Run	Factor 1 A: Laser Power (Watt)	Factor 2 B: Layer Thickness (mm)	Factor 3 C: Orientation (Deg)	Response Tensile (Mpa)
1	70	0.15	0	33.0209
2	67.5	0.09	90	36.5154
3	72.5	0.12	180	9.75328
4	67.5	0.12	0	26.0727
5	67.5	0.12	180	8.10231
6	70	0.09	180	27.5564
7	70	0.09	0	37.5419
8	70	0.15	180	15.2893
9	72.5	0.09	90	39.4278
10	72.5	0.15	90	24.5668
11	70	0.12	90	24.1492
12	70	0.12	90	24.1492
13	70	0.12	90	24.1492
14	70	0.12	90	24.1492
15	67.5	0.15	90	18.3039
16	70	0.12	90	24.1492
17	72.5	0.12	0	30.85

Table 3 Model summary statistics

Source	Lack of Fit ρ -value	Adjusted R ²	Predicted R ²	Remarks
Linear	0.0008	0.6438	0.3980	Suggested
2FI	0.8973	0.5625	-0.3886	
Quadratic	0.0026	0.9093	0.3650	Suggested
Cubic			1.0000	Aliased

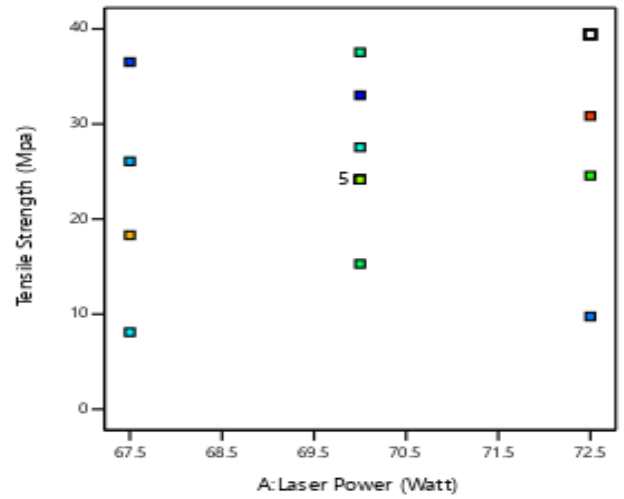


Figure 8(a). Tensile strength vs laser power.

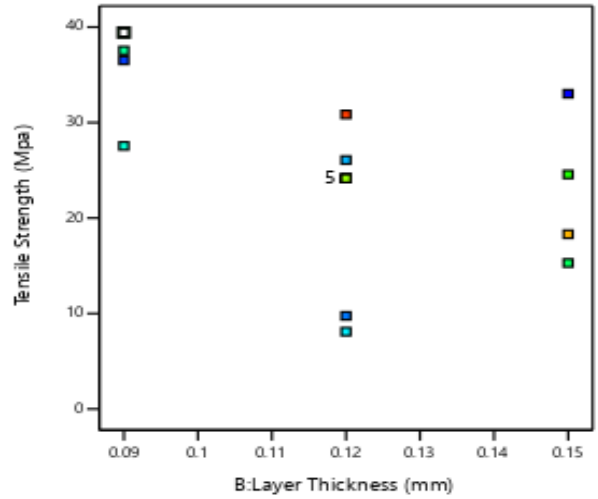


Figure 8(b). Tensile strength vs layer thickness.

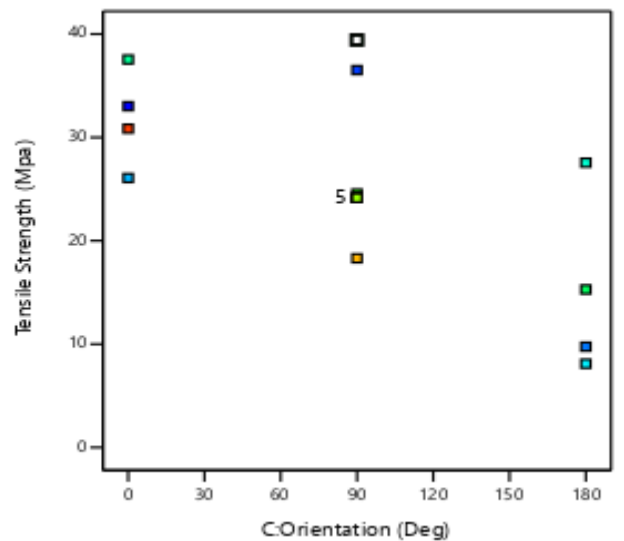


Figure 8(c). Tensile strength vs Orientation.

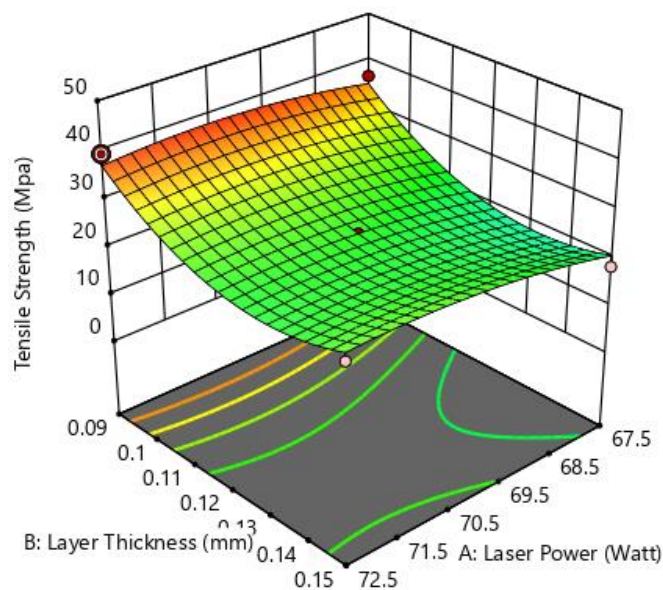


Figure 9. Effect on Tensile Strength Tensile Strength Effect.

5. CONCLUSIONS

The establishment of the proposed method optimization of recycled ageing PA-12 material for 3D Selective Laser Sintering printer effect on tensile strength by changing parameters such as laser beam power, layer thickness and part arrangement during sintering. The RSM analyses showed the highest tensile strength at 90 degree is 39.4278MPa with laser power 72.5watt and .09mm layer thickness. While the lowest tensile strength is 8.1023Mpa at 180 degree with laser power 67.5watt and layer thickness 0.12mm. The finding shows that the RSM analyses for tensile strength of recycled ageing power of polyamide-12 is lower than the value of virgin powder, which is 48.1Mpa at 0 degree with laser power 70watt and 0.12mm layer thickness [29].

ACKNOWLEDGEMENTS

This work is partially supported by Universiti Teknikal Malaysia Melaka (UteM).

REFERENCES

[1] B. Yao, Z. Li, and F. Zhu, "Effect of powder recycling on anisotropic tensile properties of selective laser sintered PA2200 polyamide," *Eur. Polym. J.*, vol. 141, p. 110093, Dec. 2020, doi: 10.1016/j.eurpolymj.2020.110093.

[2] S. C. Ligon, R. Liska, J. Stampfl, M. Gurr, and R. Mülhaupt, "Polymers for 3D Printing and Customized Additive Manufacturing," *Chemical Reviews*, vol. 117, no. 15. American Chemical Society, pp. 10212-10290, Aug. 09, 2017. doi: 10.1021/acs.chemrev.7b00074.

[3] A. Patel, V. Venoor, F. Yang, X. Chen, and M. J. Sobkowitz, "Evaluating poly (ether ether ketone) powder recyclability for selective laser sintering applications," *Polym. Degrad. Stab.*, no. xxxx, p. 109502, 2021, doi: 10.1016/j.polymdegradstab.2021.109502.

[4] A. Pilipović, T. Brajlili, and I. Drstvenšek, "Influence of processing parameters on tensile properties of SLS polymer product," *Polymers (Basel)*, vol. 10, no. 11, 2018, doi: 10.3390/polym10111208.

[5] Y. Yang, Y. Xu, S. Wei, and W. Shan, "Oral preparations with tunable dissolution behavior based on selective laser sintering technique," *Int. J. Pharm.*, vol. 593, no. November 2020, p. 120127, 2021, doi: 10.1016/j.ijpharm.2020.120127.

[6] R. Hudak, M. Šarik, R. Dadej, J. Živčák, and D. Harachová, "Material and Thermal Analysis of Laser Sintered Products", *Acta Mechanica Et Automatica*, Vol. 7, no. 1, pp. 115-19, 2013.

[7] S. Kumar, "Selective Laser Sintering: A Qualitative and Objective Approach", *JOM*, Springer-Verlag, Vol. 55, no.10, pp. 43-47, 2003.

[8] D. L. Bourell, H. L. Marcus, J. W. Barlow and J. J. Beaman, "Selective laser sintering of metals and ceramics," *Int. J. Powder Metallurgy*, Vol. 28, no. 4, pp. 369-381, 1992.

[9] A. Simchi and H. Pohl, Effects of laser sintering processing parameters on the microstructure and densification of iron powder, *Materials Science & Engineering: A*, Elsevier, Vol. 359, pp. 119-128, 2003.

[10] P. Fischer, V. Romano, H. P. Weber, N. P. Karapatis, E. Boillat, and R. Glardon, "Sintering of commercially pure titanium powder with a Nd:YAG laser source", *Acta Materialia*, Vol. 51, pp. 1651-1662, 2003.

[11] A. Ghanekar and R. Crawford, "Optimization of SLS Process Parameters using D-Optimality", *Douglas Watson National Instruments Inc*, Austin, TX, pp. 348-362, 1992.

[12] J. P. Kruth, X. Wang, T. Laoui, L. Froyen, "Lasers and materials in selective laser sintering", *Assembly Automation*, Vol. 23, no. 4, pp. 357-371, 2003.

[13] T. Laoui, X. Wang, T. H. C. Childs, J. P. Kruth, and L. Froyen, "Laser penetration in a powder bed during selective laser sintering of metal powders: simulations versus experiments", *Proc. SFFS Symp.*, Austin, pp. 7-9, 2000.

[14] J. P. Kruth, G. Levy, F. Klocke, T. H. C. Childs, "Consolidation phenomena in laser and powder-bed based layered manufacturing", *Annals of the CIRP*, Vol. 56, no. 2, pp. 730-759, 2010.

[15] S. Das, "Physical aspects of process control in selective laser sintering of metals", *Advanced Engineering Materials*, Vol. 5, pp. 701-711, 2003.

[16] T. H. C. Childs, C. Hauser, and M. Badrossamay, "Selective laser sintering (melting) of stainless and tool steel powders: experiments and modeling", *Proc. IMechE part B, J. Engineering Manufacture*, Vol. 219, pp. 339-357, 2005.

[17] S. Dimov, and D. T. Pham, "Rapid tooling applications of the selective laser sintering process", *Assembly Automation*, Vol. 21, no. 4, pp. 296-302, 2001.

- [18] K. Senthilkumaran, P. M. Pandey, and P. V. M. Rao, "Influence of building strategies on the accuracy of parts in selective laser sintering", *Materials and Design*, Vol. 30, pp. 2946-2954, 2009.
- [19] ASTM International "Standard test method for tensile properties of plastics" D638 – 10, 2010.
- [20] J. Benz, and C. Bonten, "Temperature induced ageing of PA12 powder during selective laser sintering process," in *AIP Conference Proceedings*, Jan. vol. 2055, 2019. doi: 10.1063/1.5084904.
- [21] L. Verbelen et al., "Effect of PA12 powder reuse on coalescence behaviour and microstructure of SLS parts," *Artic. Eur. Polym. J.*, 2017. doi: 10.1016/j.eurpolymj.2017.05.014.
- [22] A. D. Pradeep, T. Rameshkumar, and M. Kumar, "Parameter optimization of SLS Sinterstation 2500plus using GRA for better surface finish and dimensional accuracy," *Mater. Today, Proc.*, no. xxxx, pp. 1-5, 2021, doi: 10.1016/j.matpr.2021.01.638.
- [23] M. P. Kumar, and K. V. Kumar, K. V, "Response Surface Methodology – A Review," vol. 8, no. 7, pp. 558-565, 2020.
- [24] S. Kumar, P. Kumar, and S. H. Shan, "Effect of Process Parameters on the Solidification Time of Al-7%Si Alloy Castings Produced by VAEPD Process, *Materials and Manufacturing Processes*", Vol. 22, pp. 879-886, 2007.
- [25] M. Manohar, J. Joseph, T. Selvaraj, and D. Sivakumar, "Application of Box Behnken design to optimize the parameters for turning Inconel 718 using coated carbide tools, *International Journal of Scientific & Engineering Research*, Vol. 4, no. 4, pp. 620-642, 2013.
- [26] M. V. Satish Kumar, M. Pradeep Kumar, S. Vamshi Krishna, and K. Vikram Kumar, "Optimization of CNC Turning Parameters in Machining EN19 using Face Centered Central Composite Design Based RSM, *International Journal of Recent Technology and Engineering (IJRTE)*, ISSN: 2277-3878, Vol. 9, no. 2, 2020.
- [27] I. Sopyan, D. Gozali, Sriwidodo, and R. K. Guntina, "Design-Expert Software (Doe): an Application Tool for Optimization in Pharmaceutical Preparations Formulation," *Int. J. Appl. Pharm.*, vol. 14, no. 4, pp. 55-63, 2022. doi: 10.22159/ijap.2022v14i4.45144.
- [28] Ferreira et al., "Box-Behnken design: An alternative for the optimization of analytical methods," *Anal. Chim. Acta*, vol. 597, no. 2, pp. 179-186, 2007, doi: 10.1016/j.aca.2007.07.011.
- [29] G. Hou, H. Zhu, and D. Xie, "The Influence of SLS Process Parameters on the Tensile Strength of PA2200 Powder," *IOP Conf. Ser. Earth Environ. Sci.*, vol. 571, no. 1, 2020, doi: 10.1088/1755-1315/571/1/012111.
- [30] R. A. Hamid, S. Nur, H. Husni, and T. Ito, "Malaysian Journal on Composites Science Effect of Printing Orientation and Layer Thickness on Microstructure and Mechanical Properties of PLA Parts". Vol. 8, no. 1, pp. 11-23, 2022.
- [31] S. Pande, D. Mauchline, and D. de Beer, "Effect of Orientation on Tensile Strength of parts laser sintered with PA 12 powder". In *Proceedings of the International Conference on Additive Manufacturing and 3D printing*, Chennai, India, 6-7 February 2015.
- [32] M. R. Omar et al., "Effect of Polyamide-12 Material Compositions on Mechanical Properties and Surface Morphology of SLS 3D Printed Part," *J. Mech. Eng.*, vol. 19, no. 1, pp. 57-70, 2022. doi: 10.24191/jmeche.v19i1.19686.